Evolution of morphology through sculpting in a voxel based robot

Kathryn Walker[1] and Helmut Hauser[2]

***Abstract*— Conventional design for robotics is based on the assumption that the robot should operate only in one given environment. As a result, often their skills are not transferable. Biological systems on the other hand are surprisingly versatile and robust. They exhibit remarkable adaptivity by placing more emphasis on adapting their morphology. Consequently, providing robots with mechanisms to adapt their bodies (material properties and even removing/adding parts) could be a way to obtain more versatile and robust systems. In this paper we propose a novel method which uses genetic algorithms to evolve optimal adaptation rules for changing the bodies of soft robots. Instead of optimising the morphology directly, we optimise the rules that tell the robot how to adapt the body based on the feedback it receives when interacting with the environment. It uses a combination of local and global information to sculpt (i.e., change stiffness and remove body parts) the soft body to improve locomotion in different environments. We show that in some cases the same rule with the same starting morphology can lead to different, but beneficial morphologies in different environments, i.e., it can translate feedback from the different environments into different useful bodily changes. Furthermore, we demonstrate that some of the found rules are highly robust and are able to produce successful morphologies for a range of environments that haven't been experienced during the optimisation process.**

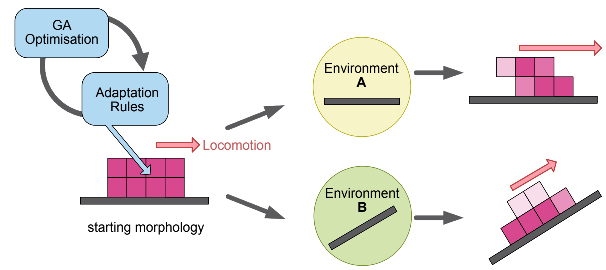

Fig. 1: General principle of the proposed approach. The chosen goal was to improve locomotion. With the help of Genetic Algorithms we optimise *adaptation rules* that translate feedback from the environment into morphological changes (i.e., changing stiffness and removal). This means, with the same starting configuration and the same adaptation rules, when the robot is exposed to different environment, it will receive different feedback and therefore sculpt into different end morphologies.

I. INTRODUCTION

Despite the success of robotics in numerous fields, robust locomotion in complex, demanding environments still remains a significant challenge. Only a few notable exceptions (such as Big Dog [28]) come close to replicating the movements we observe in biological systems. It has been suggested that this is due to the traditional constrained design approach in robotics [12]. Typically, robots are built with a predefined and fixed morphology and a corresponding suitable controller is found [26]. If a new behaviour is required, typically, only the controller is changed, but the morphology of the robot is kept as it is. This works well in traditional robotic applications where the environment is well known and can be controlled, like assembly lines or under lab conditions, but it has its limitations when complex behaviours are required to deal with unexpected situations, e.g. changes in the environment, or new tasks. The required controller becomes often too complicated and the robot is likely to fail.

The concept of *embodied intelligence* promises an alternative approach by placing higher emphasis on the morphology of the robot and its interaction with the environment [27]. Often, designing a more appropriate morphology can significantly improve the performance of a robot, whilst still employing either a very simple control system [5], or in some cases none at all [22], [35]. Many researchers have taken inspiration from this approach and used genetic algorithms to evolve optimal morphologies, see for examples [2], [4], [8], [10], [19], [30]. However, they are all optimised for one fixed environment. If the environment changes, the robot likely fails, because it does not have the ability to adapt. It's missing robustness. To solve this problem adaptive morphology (often referred to as morphosis [14]) is required. Moreover, if this adaptivity is coupled with information obtained through interaction with the environment, we obtain a highly flexible system potentially capable of optimising to a variety of situations. It seems that biological systems rely heavily on adaptive morphology. For example, in plants [11], [23] where photo-convertible molecules found in the cells can be activated by specific wave lengths of light when the cells are above ground. The light simulates growth of the stem and thus positioning leaves away from shaded areas [11], [29]. Interestingly, the same cells when submergence in water and, therefore, are stimulated differently, result in rapid growth in from of roots and they remove the leaves [32]. In these instances, the same plant genotype has been exposed

This work was supported by the EPSRC Centre for Doctoral Training in Future Robotics and Autonomous Systems (FARSCOPE) EP/L015293/1. Code available at https://github.com/kattwalker/SculptingMorphology

[1]Kathryn Walker is with IT University Copenhagen, Copenhagen, Denmark kwal@itu.dk

[2]Helmut Hauser is with both the Department of Engineering Mathematics, Bristol University, and Bristol Robotics Laboratory helmut.hauser@bristol.ac.uk

to different environments and corresponding stimuli and has reacted to them by adapting its morphology accordingly in order to survive.

Changing morphology as a reaction to external environmental stimuli occurs not only in plants but also in animals. For example, Passerine birds change their musculature to cope with low temperatures in winter [21]. The Arctic fox changes the texture and colour of its coat in response to temperature changes [23]. The tiger salamander is capable of a radical metamorphosis if its aquatic environment becomes uninhabitable, and when a male bluehead wrasse is removed from his harem, a female will change its phenotype to become a male [23]. In all these cases, the biological systems have reacted to changes in their environments (and corresponding changes of stimuli) and adapted their morphology accordingly. They have not just relied on a change in their behaviour (i.e., their control system), but have also used significant morphological changes to survive.

Inspired by these natural processes, we propose here soft robotic systems that change their morphology in response to external stimuli induced by changes in the environment (see Figure 1). We use an evolutionary algorithm to optimize rules that describe how a robot should adapt its morphology based on the feedback it gets from its interaction with the environment. Specifically, in this work the goal was to improve locomotion speed. The robot is driven by a simple control signal (i.e., contracting rhythmically a subset of its soft body) which doesn't change. Depending on the environment, the rest of the body, which is soft as well but passive, will deform in reaction to this interaction. Information on local deformation as well the overall locomotion distance will be used as input for the optimal rules to change the morphology.

The way the robot should adapt its morphology is encoded in the form of a very simple neural network. The weights of this neural network are optimised via an evolutionary algorithm. Note that adaptation is not instantaneous, instead it is employed in form of an episodic approach, where adaptation happens over a number of interactions with the environment (episodes). During each episode, the effect that the interaction with the environment has on different body parts, i.e., the kinetic energy of each part of the robots body, is recorded. At the end of each episode episode the neural network (here called sculpting adaptation system) uses this information to determine which parts to stiffen, soften or all together remove for the next attempt. Therefore, after a number of episodes, if the adaptation system has been successful, an optimal robot morphology, specifically adapted to a particular environment will have been sculpted. Evolution is carried out in three distinct environments in order to investigate transferability of optimal sculpting adaptation systems between environments, i.e., if they still able to produce a successful morphology for a new environment not experienced during optimisation.

II. Related work

The overall aim of this paper is to evolve optimal sculpting adaptation systems that use environmental stimulation to sculpt robots capable of performing (locomoting) in different environments.

There have been many examples of changing a robots control system in response to a change in environmental stimulus e.g., [9], [24], [25], [31]. In the majority of these examples the robots are controlled by a neural network, the weights of which are adapted over the lifetime of the robot. Therefore, as the robot interacts with its environment its behaviour changes, but their morphology stays fixed.

There are comparatively few examples of robots capable of changing their morphology in response to different environments. Whilst using techniques such as evolutionary algorithms to design optimal robot morphologies is not a new concept, e.g., see examples such as [2]–[4], [8], [10], [30]. However, robots capable of online morphosis is a more recent concept. For example, Bongard [1] showed that allowing some predefined development in early evolution stages (i.e., from anguilliform to legged robot) resulted in better performing and more robust final robots. Similarly, Zhu et al. [36] showed that the combination of discrete growing stages (tadpole to frog robot) and transfer learning can significantly accelerate learning control policies. Kriegman et al. [18] showed the benefits of using even a small amount of morphological adaptation, coupled with evolution, can create better performing (voxel) based robots. Initially their approach did not consider how the environment could influence growth; but touched on the idea later, in [17]. In this later work, the stiffness of each voxel was changed dependent on feedback from its interaction with the environment which was shown to increase the robustness of the evolved robots. Similarly, [7], inspired by the adaptive nature of plants, investigated how individual voxels could alter their respective size to alter the overall virtual creatures morphology. Corucci et al. [6] also investigated how a small change in morphology could result in a large behaviour change in an underwater robot named "PoseiDRONE". Here, different morphologies were able to translate the same simple (sinusoidal) control systems into different behaviours, e.g., swimming, hopping, etc. In all these cases, it was always the morphology (and/or the controller) that was optimised.

However, Walker and Hauser [33], [34] took a step further by evolving not the morphology/controller directly, but underlying adaptation rules. They studied evolving simple rule sets that adapted the morphology and control of simulated robots based on the SLIP model to increase the robustness of locomotion in response to changes in the environment. However, the used model was very simple and only 2 parameters were adapted. The presented work here takes this initial approach to much more complex structures, i.e., voxel-based soft robots, and to a range of environments to test transferability.

III. Method

This section details the used methods. First, we introduce the design of the robot, then a short discussion of the simulation software is presented. The overall simulation framework is introduced and the method used to adapt the morphology of the robot is presented. Finally, the evolutionary algorithm used to evolve the adaptation system is explained.

A. Initial Robot Design and Simulation Software

For the simulations the software Voxelyze was used, see [15] for a full description. In Voxelyze, robots are built out of 3D cubes, or voxels, connected to form a structure, in this case our robots. The starting structure of our robots was made from 216 square voxels arranged into a cube with the dimensions 6x6x6 voxels. Each voxel had a volume of 0.125m^3 and a starting stiffness of 50,000N/m, which is in the middle of the possible simulation range for the stiffness in our experiments. The density of each voxel was set to a fixed value of 1200kg/m^3.

A simple locomotion control signal was applied to the centre of the robot, as shown in Figure 2. Specifically, a central sinusoidal control signal with a period of $T = 0.25$ seconds was applied to a set of specific, so-called active voxels allowing them to expand and contract by 20% (green voxels in Figure 2). In addition, an increasing phase shift from front to back (from 0 to -0.5 rads along the y-axis) has been added to achieve locomotion. Note that this control is fixed throughout the simulation. It is not part of the optimisation process. Also note that the pink voxels are passive and, hence, are not driven by the central control signal.

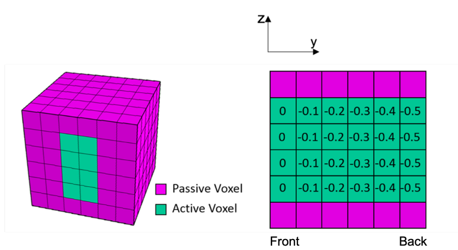

Fig. 2: The initial configuration of the robot. The inner green voxels are able to expand/contract by up to 20 percent in line with the control signal (sinusoidal, with a period of 0.25 seconds) and continue the entire way through the body of the robot. There is also a phase shift along the y-axis of the robot. The phase shift increases from front to back with each voxel, starting at 0 and ending at -0.5 rads.

B. Simulation Design

The robots were simulated for 7 seconds. This length was chosen as it allowed for a significant number of voxel expansion cycles, specifically 28 cycles, whilst still maintaining a short enough run time for efficient optimization. These 7 seconds are called an *episode*. Throughout each episode j the kinetic energy $E_{j,i}$ of each individual voxel i is recorded. Note that the kinetic energy is calculated by the formula $E_i = \frac{1}{2}m_i v_i^2$, where m_i is the mass and v_i is the resultant velocity of the ith voxel. This local information, i.e., the kinetic energy for every voxel, and the change in global distance the entire robot travels between consecutive episodes (ΔD_j) form the inputs of the sculpting adaptation system. Whilst the overall goal of this framework is to create optimal final morphologies, it is not the final morphologies that are optimised but instead the sculpting adaptation system that is evolved using an evolutionary algorithm.

The simulation process has following steps (see Figure 3). The robot is first simulated in its starting configuration (a cube with the same stiffness in all voxels, shown in Figure 2). The simulation runs for one episode, which is 28 cycles of the sinusoidal control signal (i.e., 7 seconds). During this time the kinetic energy, E, of all voxels are collected and difference between the total distance the robot travelled in the current episode and the previous (ΔD_j) recorded. Using the current sculpting adaptation system the individual change of stiffness ΔK is calculated for every voxel. The same sculpting adaptation system, which is encoded into the artificial neural network, is used for each voxel. More description of the artificial neural network is detailed in the next section. When the stiffness falls below a certain threshold, the voxel is removed (the body is "sculpted"). In the next episode, this new updated morphology is simulated for the same amount of time; the same data is recorded and the same steps are followed to adapt the morphology. After 15 episodes the process is stopped. The performance $D_{j=15}$, i.e., travelled distance in the final episode serves as performance measurement for the evolutionary algorithm.

C. Sculpting Adaptation System Design

This section details the design of the sculpting adaptation system, which dictates how the stiffness of each voxel is changed, and therefore when they are eventually removed. The sculpting adaptation system is implemented as a simple artificial neural network (ANN), shown in Figure 4a. This ANN is encoded in genomes (Figure 4b) and optimised via an evolutionary algorithm. Note that we specifically chose to use a simple neural network as our sculpting adaptation system, rather than a CPPN which is commonly used in this field, i.e., to evolve virtual creatures. To our knowledge, our work is the first example of sculpting robots after initialisation to adapt them to different environments. As a result we wanted to keep the system as simple as possible as an initial starting point to this methodology. The ANN is used to determine the stiffness change for all of the voxels in one robot using two main inputs. The first input is the change in distance travelled by the whole robot in the y-axis between two consecutive episodes ($\Delta D = D_j - D_{j-1}$) where j is the episode number. This value is the same for all voxels in the robot. The second input is the difference between the average kinetic energy across all the voxels in jth episode, E_j, and the local individual kinetic energy of the ith voxels $E_{j,i}$, i.e. $\Delta E_{j,i}$) Therefore, this input changes from voxel to voxel.

The output of the ANN is ΔK_i, i.e, how much the stiffness of the particular voxel i should be changed by. This amount is added to the existing stiffness of the corresponding voxel; if it is positive, stiffness is increased. A negative ΔK_i decreases

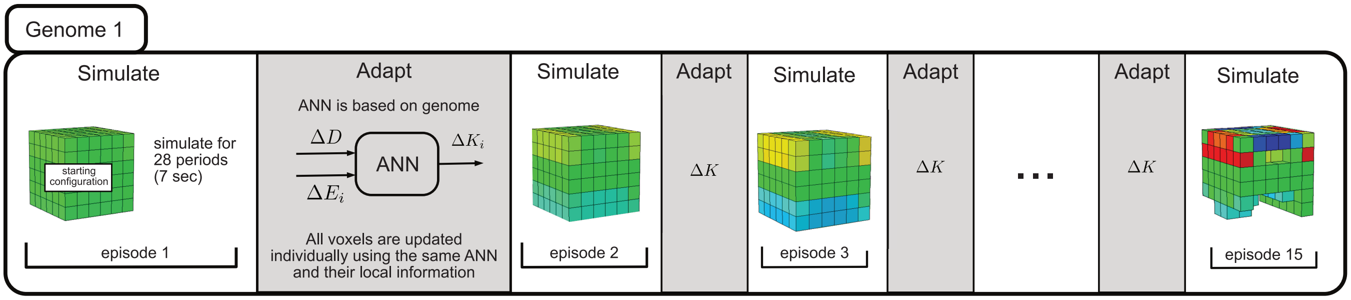

Fig. 3: This figure shows the basic method of how a suitable morphology is sculpted out of the original cube, using an evolved sculpting adaptation system. After each episode the total distance travelled is recorded as well as the individual average force in each voxel. The change in stiffness of each voxel is calculated by inputting the above values *for each voxel* into the overall control system. Note that in this figure the different colours represent the different stiffness values of each voxel, where red is the most stiff and blue the least.

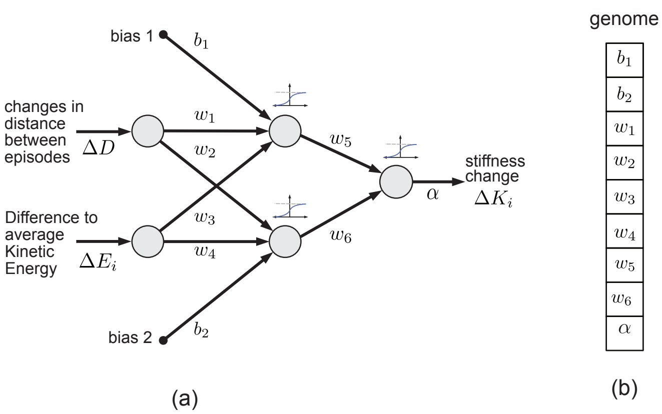

Fig. 4: This image shows the simple neural network that forms the sculpting adaptation system which is responsible for how the robot adapts between episodes. The weights of the neural network, as well as the two bias values are all optimized through the use of the evolutionary algorithm.

the stiffness. If the stiffness of an individual voxel is adjusted to below a threshold of 5000 N/m that voxel is removed, see Figure 3 for an example.

D. The Evolutionary Algorithm

This section describes the evolutionary algorithm used to evolve the sculpting adaptation systems, i.e., the ANN. Figure 4b shows the parameters used to make up the genome. In this work the structure of the neural network was kept as simple as possible to reduce the search space for the evolutionary algorithm. All parts of the genomes (i.e. the weights and biases and the learning rate, α, were constrained to take values between -1.5 and +1.5. The learning rate α was a scaling factor at the readout.

An initial population of 30 different randomised genomes was formed. As discussed before, per genome, the robot was first simulated as a complete cube of 216 voxels. Each voxel had a starting stiffness of 50,000N/m and the inner voxels were able to expand and contract, as depicted in Figure 2. After one episode the stiffness of each voxel was updated according to the neural network that was encoded in the genome. This was continued for 15 episodes, after which the distance in the final episode was recorded and used as a fitness measurement for the current genome. This process was repeated for all of the 30 randomised genomes in the initial population. Once the distance reached in the final episode was recorded for the entire population, the population was sorted accordingly to their performance, i.e., how far they have travelled in the final episode. A new population for the next generation was formed in the following way. The best genome in the current generation was transferred to the new generation unchanged. The next 17 genomes were formed by randomly selecting and mutating genomes from the current generation; to mutate, randomly generated Gaussian noise, amplitude 0.05, was added to each of the parameters in the genome. The final 12 of the new generation were randomly initialised. The evolutionary algorithm was run for 150 generations until convergence.

As mentioned in the introduction section, we aimed to find an optimal way of adaptation that works in a wide range of environments seperately. However, first we ran the genetic algorithm in three different environments, shown in Figure 5, with the goal to investigate inherent transferability between environments. Firstly, the robot was simulated on a horizontal plane (environment A), i.e. flat ground. Secondly, the environment was changed by introducing a 15 degree slope (environment B). For this environment, the robot was positioned so that the line of actuation went uphill. Finally, the evolutionary algorithm evolved sculpting adaptation systems for environment C, where the slope was remained at 15 degrees, but the robot was positioned so that it neither faced up nor down the slope. Instead, the line of actuation lay across the slope, as shown in Figure 5. The evolutionary algorithm was run 10 times in each environment with 10 unique, randomized starting populations.

IV. RESULTS

Figure 6 shows the average generational fitness (average over 10 evolution runs) for each of the three environments. A selection of the final morphologies developed in each of the three environments are shown in Figure 8. In this figure, red indicates a very stiff voxel, whereas blue indicates a

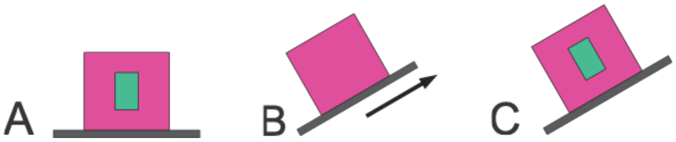

Fig. 5: Figure showing the three environments for which the sculpting adaptation system was optimized.

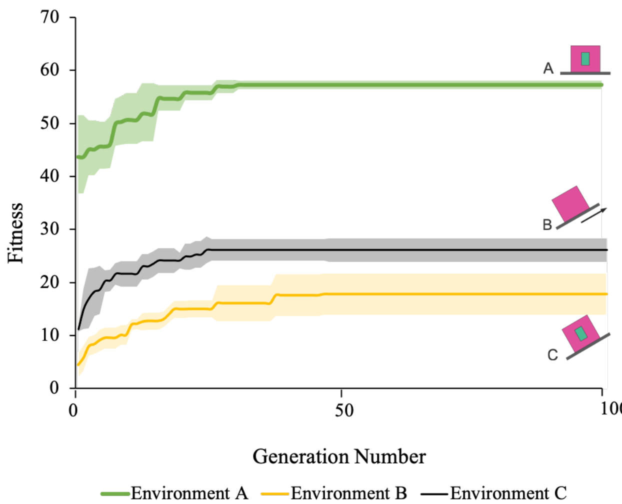

Fig. 6: Generational fitness for the best genomes evolved in the three initial environments. Also note that although the evolutionary algorithms were run for 150 generations, for readability only 100 generations are shown on the graph. Shown with 95% confidence interval

soft voxel. For Environment A, the majority of the final morphologies have a very similar overall body shape – they have a stiff top front part and stiff bottom back part, similar to those in the first and second columns. The front bottom voxels have been removed giving the illusion of ”hind legs”. The final morphologies in this environment are very successful; an unsculpted robot is only able to locomote slightly backwards (-0.61 voxels) whereas these the top genomes sculpt robots able to travel forward by 54 voxels, i.e., 9 body lengths, in a single episode.

Figure 7 shows the success of the 10 top genomes from the environment A in green. To investigate how well the genomes evolved in one environment transferred to another, the sculpting adaptation systems optimised for environment A were also tested in the other two environments. The performance in these unseen environments is also shown in the top graph of Figure 7 (gray for environment B and dark yellow for environment C). In these *transferability tests* the same starting morphology (cube) was simulated in environment B and C, but using the sculpting adaptation system (the genomes) evolved for environment A to dictate how it should adapt. This is also indicated by the black dot on the green bar. Since the kinetic energy input to

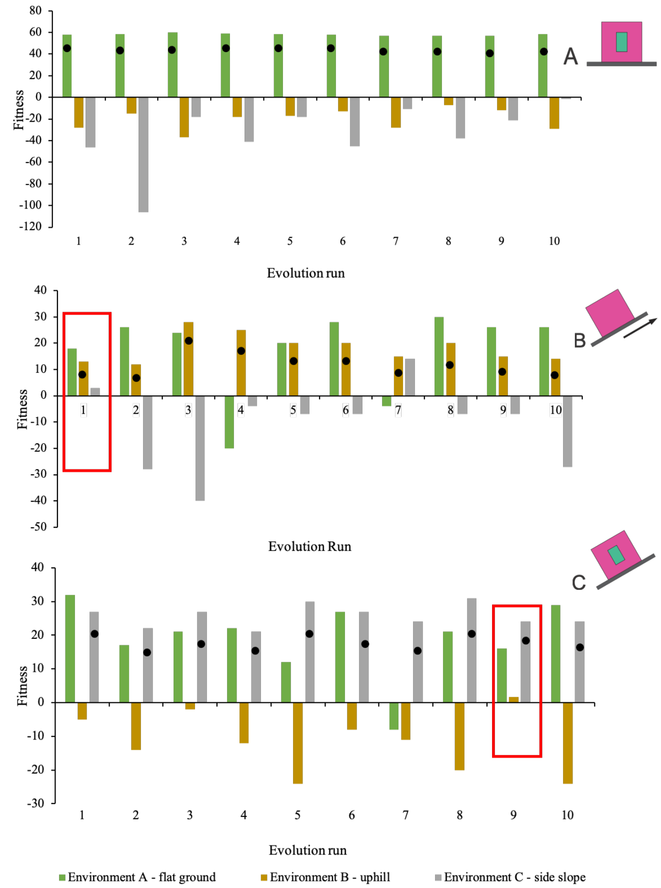

Fig. 7: Performance of the top 10 evolved genomes for each environment and tested for transferability in the other two. A black dot indicates the environment for which the sculpting adaptation system was initially evolved – this is also indicated by the diagram at the top left of each graph. A red box highlights the sculpting adaptation systems which showed transferability, i.e., they are capable of sculpting successful but different morphologies in each of the three environments. Note that the scale of the y-axis for environment A is different (compare Figure 6).

the neural network is different for each environment (i.e., the feedback), different final morphologies were sculpted. However, in this particular cases (transfer from environment A→B and A→C) this was not successful as can been seen in Figure 7 (top graph). The sculpted morphologies in these new environments either fell down hill (environment B) or turned and locomoted downhill (environment C). This is why the fitness in these environments was negative.

The morphologies developed from the top genomes found through evolution in environment B are shown in Figure 8b. In general, for this environment the obtained morphological solutions exhibited more variation. However, some final morphologies were similar to those developed in environment A, (e.g., shown in the third column of Figure 8b). They had a

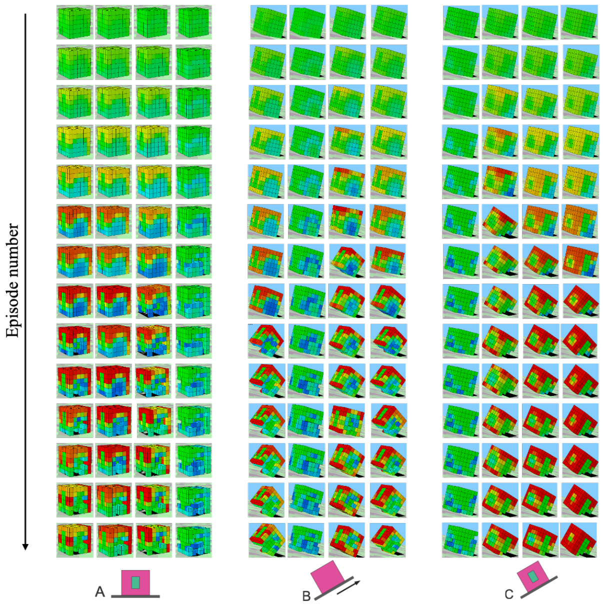

Fig. 8: The sculpting process for three example genomes in the three different environments. Note that in this figure the robots are positioned so that the front of the robot is on the right hand side of the image.

stiff front and the bottom middle voxels removed. Note that at the start of the simulation these morphologies balanced on the back voxels as a result of their interaction with the slope. When the activation of the inner voxels begins the robot fell over onto its "back" and continued locomotion from this position as shown.

Figure 7 shows the top 10 genomes which have been evolved in environment B and how they perform when tested in the other two environments. As with those found from evolution in environment A, when these genomes are simulated in environment B they perform, unsurprisingly, very well as this is the environment they were optimised for. However, with two exceptions (genomes 4 and 7), these genomes are also able to sculpt successful morphologies in environment A. This is interesting as these genomes had not experienced this environment during evolution. It might be the case that environment A is so simple, that a lot of solutions for environment B will also provide reasonably good solutions for environment A. Loosely speaking, solutions for environment A come for free when optimising for a more difficult environment like B. Additionally, there is one genome (genome 1, highlighted by the red rectangle) that is also able to sculpt a successful morphology for environment C.

Finally, we present the results from evolution in environment C. Figures 8c show the final sculpted morphologies. When compared to the morphologies obtained for environments A and B, morphologies for C show much more variation. However, one similarity they all share is asymmetry. This is expected as there is clear asymmetry in the environment and therefore in the feedback. The voxels on the right hand side of the robot (those further downhill) are either removed or are much softer than those uphill.

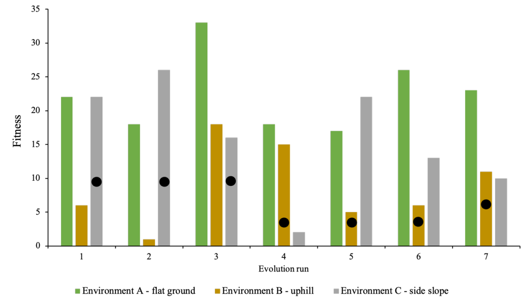

Fig. 9: The genomes from each of the three evolutionary algorithms carried out in a single environment that are able to sculpt successful morphologies in all three environments. The black dot symbolises which of the environments the genome was originally evolved for.

Figure 7 (bottom graph) shows the performance of the top 10 genomes that were optimised for environment C and their transferability to environments A and B. All of the genomes transfer well for environment A, but they fail to transfer to environment B (but for one, i.e., genome 9).

Out of the 30 genomes presented so far (the top 10 from 3 environment) only two genomes worked in all three environments, i.e., they were capable of sculpting successful morphologies in environments for which they were not optimised for. While the sculpting adaptation system is based on the environmental feedback, it doesn't optimise for transferability to new environments. The 30 genomes that have been tested are the elite – the ones that perform the highest in each particular environment. It might be they are just too specialised. To investigate this question we tested the top 50 genomes from each environment (150 genomes in total) by simulating them in the two other corresponding environments they weren't optimised for.

Figure 9 shows all genomes (in total 7) that worked in all three environments, i.e., exhibited transferabiliy. The black dot highlights which of the environments the genome was originally evolved for. Note that none of these transferable genomes were originally evolved in environment A (flat ground). Instead all transferable genomes come either from environment B or environment C. The share between them is quite equal (3 from environment C, 4 from environment B). From these results it would appear that learning an optimal sculpting adaptation system in environment A is easy, and simply evolving in a more complex environment and transferring to environment A is enough to ensure success.

To investigate how these 7 transferable sculpting adaptation systems actually change the morphology of the robots, we looked at the distance travelled at each episode, see Figure 10. Here, it can be seen that in each environment, for the first few episodes the distance travelled per episode increases gradually. When considering the corresponding sculpting figures it can be seen that in the early episodes no voxels are removed. Instead only the stiffness of the voxels change. Firstly, this shows that the performance of

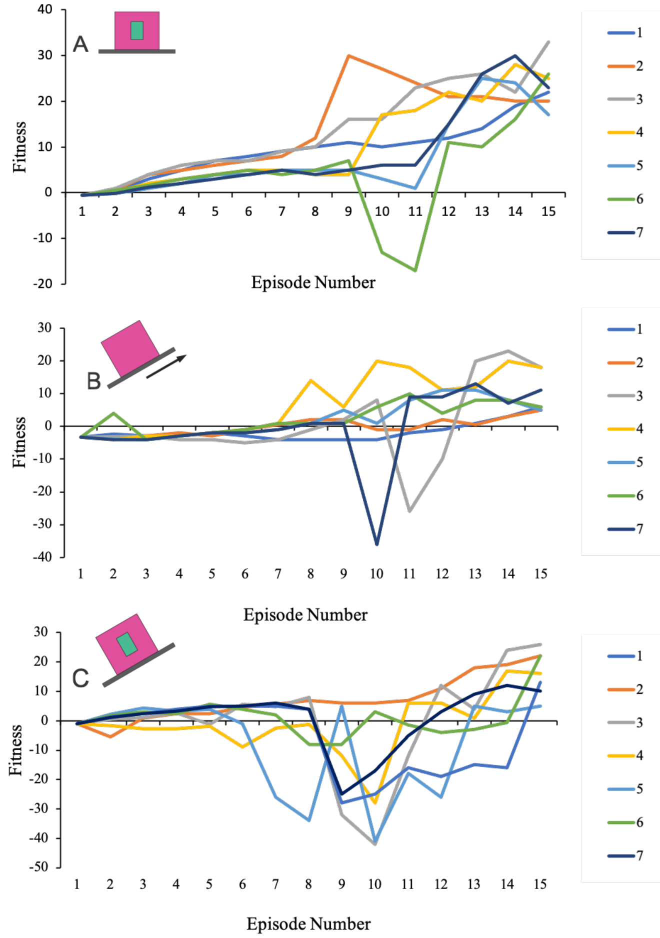

Fig. 10: Fitness of seven transferable genomes when simulated in environment A, B and C at each episode.

the robot can be improved just by altering the stiffness distribution. At approximately episode 8 (in some genomes this occurs earlier, some later) the stiffness of some voxels is decreased to the point where they are removed. In the majority of cases this temporarily results in a significant decrease in performance, especially prevalent in the more complex environments B and C. The reason for why this drop in performance in environment A is not present in most case (besides genome 6) could be the simplicity of environment A – there is no slope to roll down. So, any unbalance in the system would only cause a smaller loss in performance as opposed to environments B and C where the robot can topple and roll down the slope.

After these voxels had been removed the distance travelled per episode started to increase again. However, very few other voxels were removed. Instead the increase in performance was once again due to the change in stiffness. The voxels, especially those surrounding the removed voxels, were further stiffened. It would appear that all these sculpting adaptation systems relied on a large loss in performance (in some cases even failure) in earlier episodes in order to create final successful morphologies. The sculpting adaptation systems were able to overcome this performance drop, because they were only optimised for the performance in the final episode. Other adaptation methods like gradient descent, that were evaluated after each episode, would not able to go through this radical drop in performance, but would rather avoid it. Although adaptation through stiffness change alone did yield some improvement in performance, the combination of voxel removal and the following stiffness change seemed to be responsible for the major part of the success.

In some cases a ”zig-zagging” effect was observed, where after the initial drop in performance the fitness increases in the next episode then decreased in the one after before increasing again. This effect might haven been caused by the either the low resolution of voxels (216) or a too large scaling factor α (compare Figure 4). The robot responded too much to a change in performance and overcompensated by adjusting the stiffness too much. As a result this change in stiffness caused the robots performance to significantly change once more, again causing a large change in stiffness. On the other hand, if the scaling factor were to be reduced too much the stiffness change would be too small and therefore the performance would not be as significantly affected. Similarly if the resolution of the robot were greater, i.e., if there were more voxels, a large stiffness change of one voxel would not affect the global performance as much.

V. Discussion and Future Work

In this paper we presented a novel methodology of evolving robots that are able to adapt to new environments. This was achieved by finding optimal adaptations rules (implemented as a simple neural network) that use local kinetic energy and the global success of the robot to adjust the stiffness of discrete parts of the robot, and remove these parts if the stiffness becomes too soft. As a result, based on the feedback from the environment, successful morphologies were sculpted.

To find an optimal sculpting adaptation system we used an evolutionary algorithm. We investigated three environments separately to investigate transferability. Analysing the successful genomes from the individual environments, it was found that a small percentage (5%) showed good transferability. These genomes were able to sculpt successful morphologies in all three environments, including the two that have not been seen during the optimisation process. Furthermore, in nearly all cases, evolution in the two more complex environments (environments B and C) yielded sculpting adaptation systems capable of creating successful morphologies in the easier environment A (flat ground).

Future work will include to find more transferable sculpting adaptation systems through optimisation for all three environments simultaneously, i.e., where the fitness is the weighted sum total of the distance travelled in all three environments. The results can be then tested in additional environments. Furthermore, the investigation about the ”difficulty” of an environment would interesting to conduct. Can we find a metric that capture this complexity and can this help us to build ideal environment for robots to learn as transferable skills as possible? Additionally, in the experiments here we purposefully use a simple neural network as a sculpting adaptation rules. As discussed, this paper is the first exploration into sculpting robot morphologies. Therefore, we were motivated to keep the system as simple as possible, and explore its potential and also limitations. Therefore, future work will also include incorporating a CPPN-NEAT approach into our existing methodology. Finally, a transferability also suggest robustness. We assume such a system would be also able to recover from insult, which is currently being investigated.

The presented results are a step to bring us closer to more adaptive robotics systems. Although these results are carried out in simulation, recent advancement of sim-to-real robotics, e.g. [13], [16], [20] are promising we might be able in the near future to build robots that are capable of morphological changes and which could take advantage of our proposed approach..

ACKNOWLEDGMENT

This work was supported by the EPSRC Centre for Doctoral Training in Future Robotics and Autonomous Systems (FARSCOPE) EP/L015293/1.

REFERENCES

[1] J. Bongard. Morphological change in machines accelerates the evolution of robust behavior. *Proceedings of the National Academy of Sciences*, 108(4):1234–1239, 2011.

[2] J. C. Bongard and R. Pfeifer. Repeated structure and dissociation of genotypic and phenotypic complexity in artificial ontogeny. In *Proceedings of the 3rd Annual Conference on Genetic and Evolutionary Computation*, pages 829–836. Morgan Kaufmann Publishers Inc., 2001.

[3] N. Cheney and H. Lipson. Topological evolution for embodied cellular automata. *Theoretical Computer Science*, 633:19–27, 2016.

[4] N. Cheney, R. MacCurdy, J. Clune, and H. Lipson. Unshackling evolution: evolving soft robots with multiple materials and a powerful generative encoding. *ACM SIGEVOlution*, 7(1):11–23, 2014.

[5] S. Collins, A. Ruina, R. Tedrake, and M. Wisse. Efficient bipedal robots based on passive-dynamic walkers. *Science*, 307(5712):1082–1085, 2005.

[6] F. Corucci, M. Calisti, H. Hauser, and C. Laschi. Novelty-based evolutionary design of morphing underwater robots. In *Proceedings of the 2015 annual conference on Genetic and Evolutionary Computation*, pages 145–152, 2015.

[7] F. Corucci, N. Cheney, S. Kriegman, J. Bongard, and C. Laschi. Evolutionary developmental soft robotics as a framework to study intelligence and adaptive behavior in animals and plants. *Frontiers in Robotics and AI*, 4:34, 2017.

[8] F. Dellaert and R. D. Beer. A developmental model for the evolution of complete autonomous agents. In *Proceedings of the Fourth International Conference on Simulation of Adaptive Behavior*, pages 393–401. MIT Press Cambridge, MA, 1996.

[9] P. Dürr, C. Mattiussi, A. Soltoggio, and D. Floreano. Evolvability of neuromodulated learning for robots. In *2008 ECSIS Symposium on Learning and Adaptive Behaviors for Robotic Systems (LAB-RS)*, pages 41–46. IEEE, 2008.

[10] P. Eggenberger. Evolving morphologies of simulated 3D organisms based on differential gene expression. In *Proceedings of the Fourth European Conference on Artificial Life*, pages 205–213, 1997.

[11] K. A. Franklin. Shade avoidance. *New Phytologist*, 179(4):930–944, 2008.

[12] M. Garrad, J. Rossiter, and H. Hauser. Shaping behavior with adaptive morphology. *IEEE Robotics and Automation Letters*, 3(3):2056–2062, 2018.

[13] H. Hauser. Resilient machines through adaptive morphology. *Nature Machine Intelligence*, 1(8):338–339, 2019.

[14] H. Hauser and F. Corucci. Morphosis—taking morphological computation to the next level. In *Soft Robotics: Trends, Applications and Challenges*, pages 117–122. Springer, 2017.

[15] J. Hiller and H. Lipson. Dynamic simulation of soft multimaterial 3d-printed objects. *Soft Robotics*, 1(1):88–101, 2014.

[16] S. Kriegman, D. Blackiston, M. Levin, and J. Bongard. A scalable pipeline for designing reconfigurable organisms. *Proceedings of the National Academy of Sciences of the United States of America*, 2020.

[17] S. Kriegman, N. Cheney, and J. Bongard. How morphological development can guide evolution. *Scientific Reports*, 8(1):1–10, 2018.

[18] S. Kriegman, N. Cheney, F. Corucci, and J. C. Bongard. A minimal developmental model can increase evolvability in soft robots. In *Proceedings of the Genetic and Evolutionary Computation Conference*, pages 131–138, 2017.

[19] S. Kriegman, N. Cheney, F. Corucci, and J. C. Bongard. Interoceptive robustness through environment-mediated morphological development. In *Proceedings of the Genetic and Evolutionary Computation Conference*, pages 109–116. ACM, 2018.

[20] S. Kriegman, S. Walker, D. Shah, M. Levin, R. Kramer-Bottiglio, and J. Bongard. Automated shapeshifting for function recovery in damaged robots, 2019.

[21] E. T. Liknes and D. L. Swanson. Phenotypic flexibility of body composition associated with seasonal acclimatization in passerine birds. *Journal of Thermal Biology*, 36(6):363–370, 2011.

[22] T. McGeer et al. Passive dynamic walking. *I. J. Robotic Res.*, 9(2):62–82, 1990.

[23] A. P. Moczek, S. Sultan, S. Foster, C. Ledón-Rettig, I. Dworkin, H. F. Nijhout, E. Abouheif, and D. W. Pfennig. The role of developmental plasticity in evolutionary innovation. *Proceedings of the Royal Society B: Biological Sciences*, 278(1719):2705–2713, 2011.

[24] E. Najarro and S. Risi. Meta-learning through hebbian plasticity in random networks. *arXiv preprint arXiv:2007.02686*, 2020.

[25] P.-Y. Oudeyer and L. B. Smith. How evolution may work through curiosity-driven developmental process. *Topics in Cognitive Science*, 8(2):492–502, 2016.

[26] R. Pfeifer, F. Iida, and J. Bongard. New robotics: Design principles for intelligent systems. *Artificial Life*, 11(1-2):99–120, 2005.

[27] R. Pfeifer, F. Iida, and M. Lungarella. Cognition from the bottom up: on biological inspiration, body morphology, and soft materials. *Trends in Cognitive Sciences*, 18(8):404–413, 2014.

[28] M. Raibert, K. Blankespoor, G. Nelson, and R. Playter. Bigdog, the rough-terrain quadruped robot. *IFAC Proceedings Volumes*, 41(2):10822–10825, 2008.

[29] J. Schmitt, J. R. Stinchcombe, M. S. Heschel, and H. Huber. The adaptive evolution of plasticity: phytochrome-mediated shade avoidance responses. *Integrative and Comparative Biology*, 43(3):459–469, 2003.

[30] K. Sims. Evolving 3D morphology and behavior by competition. *Artificial Life*, 1(4):353–372, 1994.

[31] K. O. Stanley, B. D. Bryant, and R. Miikkulainen. Evolving adaptive neural networks with and without adaptive synapses. In *The 2003 Congress on Evolutionary Computation, 2003. CEC'03.*, volume 4, pages 2557–2564. IEEE, 2003.

[32] L. Voesenek, T. Colmer, R. Pierik, F. Millenaar, and A. Peeters. How plants cope with complete submergence. *New Phytologist*, 170(2):213–226, 2006.

[33] K. Walker and H. Hauser. Adapting stiffness and attack angle through trial and error to increase self-stability in locomotion. *Journal of biomechanics*, 87:28–36, 2019.

[34] K. Walker and H. Hauser. Evolving optimal learning strategies for robust locomotion in the spring-loaded inverted pendulum model. *International Journal of Advanced Robotic Systems*, 16(6):1729881419885701, 2019.

[35] M. Wisse, A. L. Schwab, and F. C. Van Der Helm. Passive dynamic walking model with upper body. *Robotica*, 22(6):681, 2004.

[36] Y. Zhu, J. Rossiter, and H. Hauser. *Learning in Growing Robots: Knowledge Transfer from Tadpole to Frog Robot*, volume 11556 LNAI. 2019.